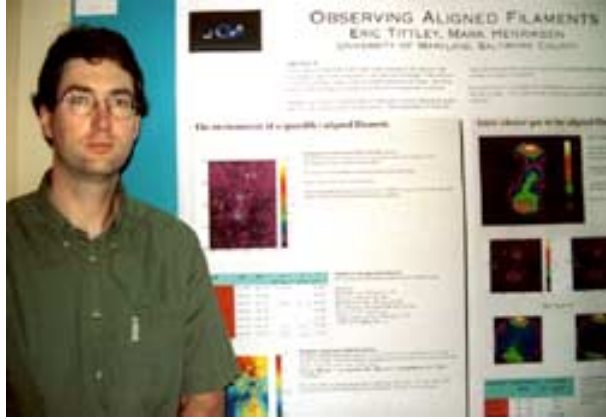


OBSERVING ALIGNED FILAMENTS



Eric Tittley and Mark Henriksen
Physics Department, University of Maryland, Baltimore County
1000 Hilltop Circle, Baltimore, MD 21250 USA

Gas residing in filaments in the large-scale structure of the universe may contribute a significant component to the total baryon budget of the universe as well as provide a supply of gas to nearby galaxy cluster halos. However, the gas will be difficult to observe if it has a low temperature or density. Filament gas may be easier to observe if the gas is viewed aligned along the line of sight, increasing the column density. Such alignments of filaments may have already been observed and mis-classified as interacting or merging systems of clusters of galaxies. Presented here is a candidate for a filamentary structure that is aligned along the line of sight. *ASCA* data reveals intercluster emission within this structure.

1 The environment of a (possibly) aligned filament

The pair of galaxy clusters Abell 3391 and Abell 3395 is associated with 3 other objects which, together, form a loose association that possesses a filamentary structure. A case may be made to separate A3395 into three components which are believed to be undergoing a merging event. However, measurements of the temperature of the intercluster medium between these components reveals little or none of the heating that would be expected from a merging event¹. The details of the separate components are listed in Table 1. Data are from references^{2, 3, 4, 5, 6, 7,} and⁸.

The x-ray emission from these members, as recorded by *ROSAT* during its All Sky Survey (ASS), is given in Figure 1. The ASS events data were used to create a flux map by finding the radii encompassing a fixed number of events (100) and using this to infer a local density for the events rate. The white circles are centred on the objects listed in Table 1. There is clear north-north-westerly trend. Note incidently the absence of emission from AS0584 (second circle from the top-right), despite it being a cD-dominated group/cluster of galaxies.

The components are located in a narrow range of redshift space, spanning just 1500 km s^{-1} . This corresponds to a redshift depth of $15h^{-1} \text{ Mpc}$ while 1° corresponds to $2.6h^{-1} \text{ Mpc}$ (at 15000 km s^{-1}). Hence, the structure is on the order of 3 times deeper in the radial direction than the tangential, if the unknown bulk motions of the components are presumed to be small (a potentially fatal flaw).

For Figure 2, the galaxy spatial distribution (contours) is derived from the list of galaxies with available redshifts⁷ from NED. The mean redshift of the galaxies is given by the colour

Table 1: Members of the supercluster/filament. The members are listed from northern-most to southern-most.

Obj	RA	Dec	L_x $10^{43} \text{erg s}^{-1}$	T keV	V_r km s^{-1}
MS 0620.6 - 5239	$6^h 21^m 44^s$	$-52^\circ 41'$	2.6 ± 0.6		15 000
AS0584	$6^h 22^m 58^s$	$-53^\circ 36'$			14 100
A3391	$6^h 26^m 15^s$	$-53^\circ 41'$	16 ± 2	4 - 5	16 500
ESO161 - IG 006	$6^h 26^m 06^s$	$-54^\circ 02'$			15 600
A3395 NW	$6^h 26^m 35^s$	$-54^\circ 20'$			14 500
A3395 E	$6^h 27^m 37^s$	$-54^\circ 27'$	$5.7^{+2.9}_{-0.4}$	$4^{+\infty}_{-4}$	15 000
A3395 SW	$6^h 26^m 49^s$	$-54^\circ 33'$	$4.2^{+5.8}_{-0.5}$	$5^{+\infty}_{-3}$	15 400

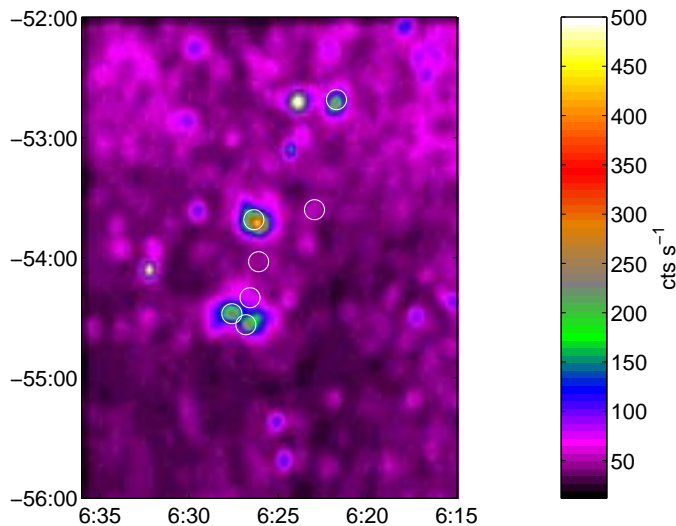


Figure 1: The field structure from the *ROSAT* All-Sky-Survey.

background image. (*ignore colours beyond the outer contour lines.*) Note that 1000 km s^{-1} corresponds to $10h^{-1} \text{ Mpc}$. The white circles are centred on the objects listed in Table 1. The large black circle corresponds to the *ASCA* GIS field of view displayed in Figure 3.

Figure 2 shows that the southern edge of the proposed filament is the closer end.

2 Inter-cluster gas in the aligned filament?

Since the proposed filamentary structure may be tilted to the line of sight such that it is being observed close to lengthwise, the column density of any intercluster gas will be higher due to the increased optical path length. Consequently the system provides a good opportunity to observe the x-ray emission from the hot intercluster medium.

The region between the two largest clusters (A3391 and A3395) was observed by *ASCA*. The data were extracted from the archive. To produce the image in Figure 3, the events data were converted to an image via an adaptive smoothing kernel which determines the local surface density of events by smoothing over a radius which encompasses a constant number (100) of events. This preliminary image was then convolved with a Gaussian with a HWHM of $1''$ (*ASCA* HPD= $2.9''$). A background count rate derived from the database of source-removed exposures

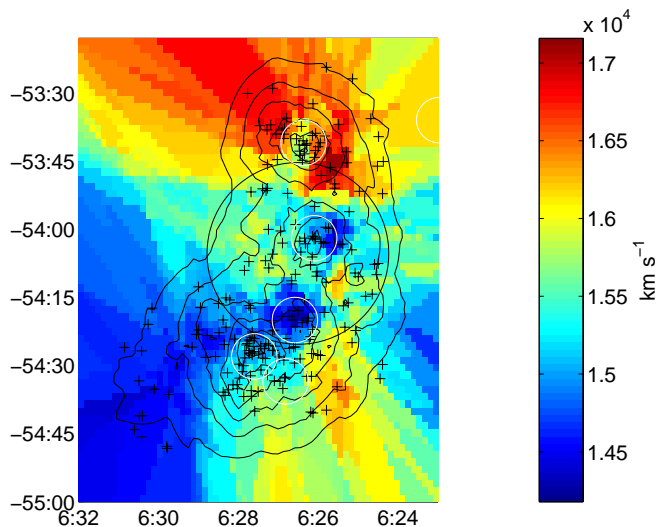


Figure 2: The galaxy spatial and redshift distribution.

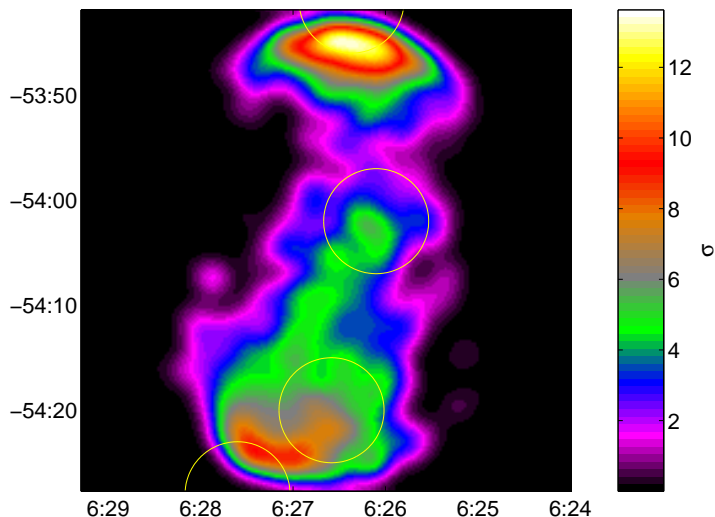


Figure 3: *ASCA* GIS image of the region between A3391 and A3395.

was subtracted. The colour scale is in units of σ above the background.

There is an enhanced count rate extending north-north-westerly from A3395, in the same orientation as the rest of the proposed filamentary structure. The rate is better than 4σ over and distance of 1.5° and terminates at the galaxy group.

Scattered photons from the bright surrounding galaxy clusters is a potential explanation for the excess count-rate between A3391 and A3395. To determine the extent of this effect, ray-tracing simulations of the field were performed. As a template, the ASS data were used; in one instance, the input count-rate in the region between the clusters was flattened to the approximate background rate.

The ray-tracing tool, `TRACE_ASCA`⁹, was used to perform the simulations.

The results of the ray-tracing are shown in Figure 4. Panels a) and b) are the input fields, and c) and d) are the respective outputs which may be compared with Figure 3. Though there is a contribution of scattered light to the centre of the field of view, it has neither the magnitude nor extend as is observed. Hence, it is unlikely that the region of extended count rate observed in the *ASCA* data between the clusters is an artefact of scattered photons. Instead, it likely

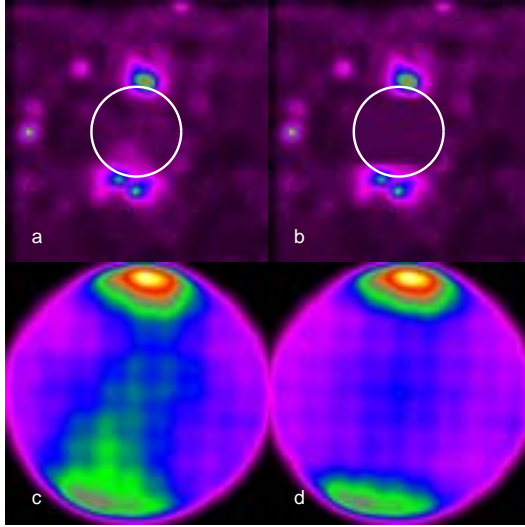


Figure 4: Ray-traced images of the *ASCA* GIS FOV.

Table 2: Computed flux rates for the intercluster emission.

Instrument	Energy window keV	X-ray flux $10^{-13}\text{erg cm}^{-2}\text{s}^{-1}$
<i>ASCA</i> GIS	0.8 - 9.0	13 ± 1
<i>ASCA</i> SIS	1.0 - 2.2	5 ± 2
<i>ROSAT</i> PSPC	0.8 - 1.8	4.9 ± 0.4

corresponds to an excess of x-ray emission.

Along with the *ASCA* GIS and SIS data, *ROSAT* PSPC data were also available in the archives which covered the A3391-A3395 intercluster region, serendipitously observed during an observation of A3395. The count rates for the region of extended emission were converted to flux rates (assuming a 1 keV temperature and a Raymond-Smith spectral model). The rates are given in Table 2. The rate for the GIS observation, at a distance of $150 h^{-1}$ Mpc, corresponds to a luminosity, $L=3.5 \times 10^{42} h^{-2} \text{erg s}^{-1} [0.8 - 9.0 \text{keV}]$. The errors include the deviation in the background rate, so the GIS detection is on the order of a 10σ detection, while the SIS comes in at less than 3σ (on its own, compatible with a null detection).

3 Conclusions

The lengthwise alignment of a filamentary structure at least three separate galaxy clusters as provided the opportunity to observe the intercluster gas within a filamentary environment.

The gas is found to extend at least $4h^{-1}$ Mpc and has a luminosity of $(3.5 \pm 0.5) \times 10^{42} h^{-2} \text{erg s}^{-1} [0.8 - 9.0 \text{keV}]$.

Scattered photons are unable to explain the observed count-rate.

References

1. Markevitch, M., Forman, W. R., Sarazin, C. L., & Vikhlinin, A. 1998, *ApJ*, 503, 77

2. De Grandi, S., Bohringer, H., Guzzo, L., Molendi, S., Chincarini, G., Collins, C., Cruddace, R., Neumann, D., Schindler, S., Schuecker, P., & Voges, W. 1999, *ApJ*, 514, 148
3. Gioia, I. M., Maccacaro, T., Schild, R. E., Stocke, J. T., Liebert, J. W., Danziger, I. J., Kunth, D., & Lub, J. 1984, *ApJ*, 283, 495
4. Henriksen, M. & Jones, C. 1996, *ApJ*, 465, 666
5. Irwin, J. A., Bregman, J. N., & Evrard, A. E. 1999, *ApJ*, 519, 518
6. Stocke, J. T., Morris, S. L., Gioia, I. M., Maccacaro, T., Schild, R., Wolter, A., Fleming, T. A., & Henry, J. P. 1991, *ApJS*, 76, 813
7. Teague, P. F., Carter, D., & Gray, P. M. 1990, *ApJS*, 72, 715
8. Tritton, K. P. 1972, *MNRAS*, 158, 277
9. Ptak, A. F. 1997, PhD thesis, University Of Maryland College Park